Organic & Biomolecular Chemistry

Cite this: *Org. Biomol. Chem.*, 2011, **9**, 6402

www.rsc.org/obc

PAPER

Theoretical investigation on mechanism of asymmetric Michael addition of malononitrile to chalcones catalyzed by *Cinchona* alkaloid aluminium(III) complex†

Zhishan Su, Hai Whang Lee and Chan Kyung Kim*

Received 24th April 2011, Accepted 17th June 2011
DOI: 10.1039/c1ob05642e

The mechanism of Michael addition of malononitrile to chalcones catalyzed by *Cinchona* alkaloid aluminium(III) complex has been investigated by DFT and ONIOM methods. Calculations indicate that the reaction proceeds through a dual activation mechanism, in which Al^{III} acts as a Lewis acid to activate the electrophile α,β-unsaturated carbonyl substrate while the tertiary amine in the *Cinchona* alkaloid works as a Lewis base to promote the activation of the malononitrile and deprotonation. A stepwise pathway involving C–C bond formation followed by proton transfer from the catalyst to the carbonyl substrate is adopted, and latter step is predicted to be the rate-determining-step in the reaction with an energy barrier of 12.4 kcal mol^{-1}. In the absence of the Al^{III}-complex, a *Cinchona* alkaloid activates the carbonyl substrate by a hydrogen bonding of the hydroxyl group, involving a higher energy barrier of 30.4 kcal mol^{-1}. The steric repulsion between the phenyl group attached to the carbonyl group in the chalcone and isopropoxyl groups of the Al^{III}-complex may play an important role in the control of stereoselectivity. The π–π stacking effect between the quinuclidine ring of the quinine and the phenyl group of the chalcones may also help the stabilization of the preferred molecular complex. These results are in agreement with experimental observations.

Introduction

The asymmetric catalytic Michael addition of carbanion nucleophiles to α,β-unsaturated carbonyl compounds represents one of the most important carbon–carbon bond-forming reactions in organic chemistry.[1–3] Nucleophiles such as malonate esters,[2c,4] diketones,[5] keto esters[5b,d,6] and nitroalkanes[7] have been extensively used to produce diversely functionalized and synthetically useful chiral adducts. Among the various nucleophiles, malononitrile is a classic equivalent of the 1,3-dicarbonyl compounds, in which the nitrile groups can be transformed into carboxylic acids,[8] esters[9] and amines.[2d,8a,10] However, the use of malononitrile as a donor in conjugate addition has received much less attention[3,11] and theoretical investigations on the mechanism involved remain limited.[12]

For Michael addition of malononitrile, organocatalysts have gained much interest.[11d–j] Bifunctional thiourea-catalyzed Michael reactions have been developed successfully, in which the thiourea moiety of the catalysts could act as a Brønsted acid and interact with the substrate through hydrogen bonding, resulting in the enhancement of its electrophilicity. Meanwhile, the aliphatic tertiary amine unit can act as a Brønsted base to deprotonate and activate the malononitrile by forming a hydrogen bond with its anion.[11e,f,h] Binary complexes between the *N*-acylpyrrolidine and thiourea involving bidentate hydrogen-bond interaction have been confirmed by ^{1}H NMR experiments.[11e] Based on the experimental observations, DFT investigations indicate that the reaction mechanism consists of three elementary steps: catalyst protonation, C–C bond coupling and catalyst deprotonation. The C–C bond coupling step has been identified as the energetic bottleneck in the reaction channel.[12]

Besides thiourea catalysts, *Cinchona* alkaloids and their derivatives have also proved to be highly effective and versatile organocatalysts in the Michael addition of malononitrile.[11g,i] The basic tertiary amine nitrogen of the quinuclidine ring moiety is thought to deprotonate the pro-nucleophile, malononitrile, leading to an increase in nucleophilicity. Carbonyl substrates can be activated by generating reactive iminium ion intermediates through the primary amine group of *Cinchona* alkaloids[11g,j] or by a hydrogen-bonding interaction between the secondary hydroxyl group of *Cinchona* alkaloids and the carbonyl compounds.[11i]

Based on the 'double catalytic activation (DCA)' concept,[13] chiral Lewis acid catalysts containing cationic transition metal or their complexes have been introduced to activate electrophiles by a coordination interaction in the Michael addition reactions by Kanemasa and his colleagues. The products with high yield and satisfactory enantioselectivities can be obtained by the use of both (*R*,*R*)-DBFOX/Ph·$Ni(ClO_4)_2$·$3H_2O$ and amine

Department of Chemistry, Inha University, Incheon, 402-751, Korea. E-mail: kckyung@inha.ac.kr; Fax: +82-32-8739333; Tel: +82-32-8607684

† Electronic supplementary information (ESI) available: Optimized geometries and energies in gas phase and toluene solvent, evolution of charge populations on carbonyl groups in the formation of the C–C bond. See DOI: 10.1039/c1ob05642e

catalysts under DCA conditions.[11a] The (*R*,*R*)-DBFOX/Ph cationic complexes of Ni(II) and Co(II) salts can successfully activate substituted malononitrile in alcohol, inducing the enantioselective tertiary/quaternary and quaternary/quaternary carbon–carbon bond formation.[11c]

Recently, Feng *et al.* have verified experimentally that the quinine-Al(O*i*Pr)$_3$ complexes are effective for the enantioselective Michael addition of malononitrile to chalcones, affording products in high yield and excellent enantioselectivity (up to 97% yield and 93% ee).[3] In contrast, alkaloid alone without Al reagents exhibited inferior results compared to those of the Al(III)–quinine systems (only 39% yield with 69% ee was obtained). Based on experimental observations, a possible dual activation mechanism model is suggested, in which Al^{III} coordinates with the oxygen atom of the hydroxyl group of *Cinchona* alkaloids and works as a more effective Lewis acid centre to activate the carbonyl group of chalcone.[3]

Theoretical investigations aimed at the nature of the real catalytic processes based on a quantum chemistry approach have proved to be a useful tool.[14] DFT calculations, in particular those using the B3LYP method, have proved effective in probing the differential interactions in diastereomeric TSs that contribute to the vital energy differences responsible for enantioselectivity in these reactions.[14,15] To understand the mechanism of the Michael addition reaction between malononitrile and chalcones, and get useful information on the asymmetric induction of the Lewis acid, theoretical investigations on the detailed mechanism of Michael addition of malononitrile to chalcones catalyzed by *Cinchona* alkaloid–Al(O*i*Pr)$_3$ complexes were performed with the B3LYP[16] and ONIOM[17] methods in the present work.

Computational details

For the present system, a complete DFT analysis would be difficult, owing to very bulky structural elements. Therefore, models were employed to probe the mechanism of the Michael addition of malononitrile and chalcones catalyzed by CI–Al(O*i*Pr)$_3$ complexes (as shown in Scheme 1).

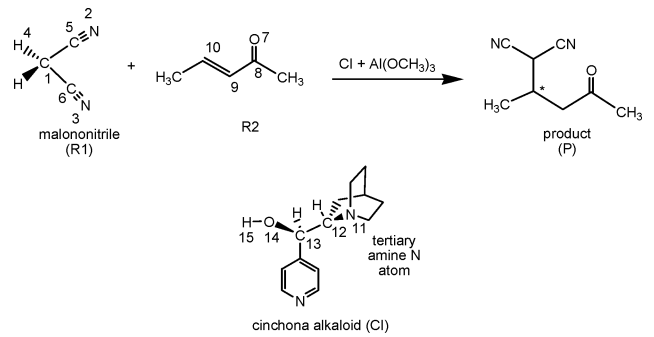

Scheme 1 Model system for the Michael addition reaction.

For the model system, all calculations were performed with the hybrid DFT method, B3LYP, as implemented in the Gaussian 03 program package.[18] Geometries were fully optimized with the 6-31++G** basis set and characterized by frequency analysis. The intrinsic reaction coordinate (IRC) path was traced in order to check the energy profiles connecting each transition state to the two associated minima of the proposed mechanism.[19] Natural Bond Orbital (NBO)[20] analysis was performed to obtain further insight into the electronic properties of the system. To understand the mechanism of reaction, DFT analysis based on the reactivity indices (electrophilicity index ω and nucleophilicity index N)[21,22] of the reactants involved in C–C bond formation was also performed by computing the B3LYP/6-31++G** HOMO and LUMO energies at the ground-state of the molecules involved. The calculated total energies and relative energies for stationary points corresponding to reactants are listed in Table S1 in the Supporting Information.† The effect of toluene solvent on the reaction was considered by employing the self-consistent reaction field (SCRF) method based on the polarized continuum model (PCM)[23] at the B3LYP/6-31++G** level. Unless otherwise specified, the Gibbs free energies corrected by both solvation and zero-vibrational effect were used in the discussion. Furthermore, Atoms In Molecules (AIM) was used to infer the existence, or otherwise, of a molecular interaction for some key intermediates in the reaction. In AIM theory, the interaction between two atoms is revealed by the presence of a charge density in the interconnection space and this charge density is related to a bond critical point (BCP). If a (3,–1) BCP existed between any pair of nuclei, these nuclei were considered to be bonded to one another.[24]

Based on the results obtained from the model system, the actual reaction was further considered. With a view to reducing computational costs, the ONIOM method was used to simulate the asymmetric reaction system in the present study (the layering of the system is shown in Scheme 2). The internal region was treated with the hybrid functional B3LYP and 6-31++G** basis set. The remainder of the system was optimized at the HF/STO-3G level. The bonds between atoms in the core and outer layers were broken and then saturated by hydrogen atoms (link atoms) for the higher level part of the ONIOM calculation on the core system. Each transition state was characterized by an analysis of the vibrational mode corresponding to its unique imaginary frequency. The calculated total energies and relative energies for stationary points corresponding to the reactants are listed in Table S2 in the Supporting Information.†

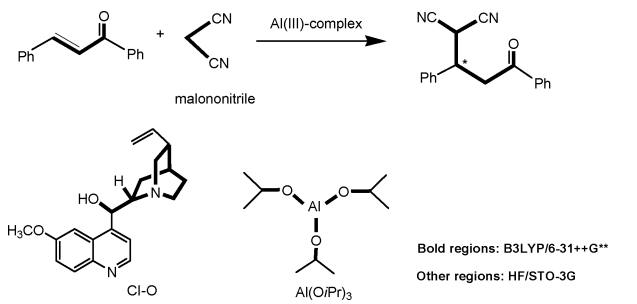

Scheme 2 Layering of the actual system for the Michael addition reaction.

Results and discussion

Isomerization and deprotonation of malononitrile catalyzed by *Cinchona* alkaloid

The generally accepted mechanism for the activation of malononitrile starts with deprotonation of malononitrile by amine base, forming an ion pair structure.[12] Calculations indicate that the

tertiary amine N atom of CI could abstract the acidic hydrogen atom from malononitrile to produce a $^{-}CH(CN)_2$ anion with high nucleophilicity (Scheme 3), promoting C–C bond coupling.

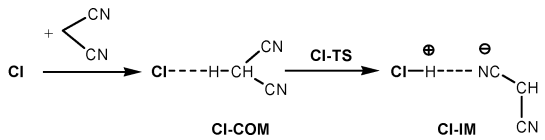

Scheme 3 Isomerization and deprotonation of malononitrile catalyzed by *Cinchona* alkaloid (**CI**).

Initially, malononitrile (**R1**) is loosely bonded to **CI** by hydrogen bonding with a slightly positive complexation free energy (6.8 kcal mol^{-1}), forming the molecular complex, **CI–COM** (Fig. 1). The N11–H4 and H15–N3 distances are 2.112 and 2.491 Å, respectively. The C1–H4 bond is slightly weakened with the increase in C–H bond length from 1.097 to 1.117 Å. In the following step, H4 transfers from C1 to N11 atoms *via* the transition state **CI–TS**. The free energy barrier is predicted to be 13.5 kcal mol^{-1}, which is similar to those of theoretical investigation on the thiourea-catalyzed Michael addition reaction by Zhang *et al.*[12] Such a lower barrier indicates that the quinuclidine moiety of the alkaloid is highly efficient for the isomerization and deprotonation of malononitrile.

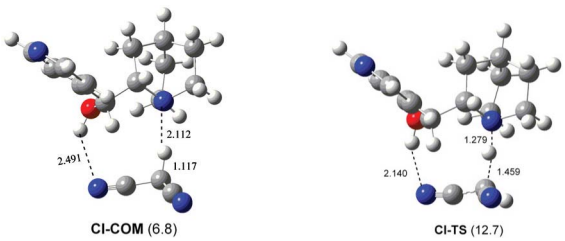

Fig. 1 Optimized geometries of molecular complex and transition states for malononitrile isomerization and deprotonation catalyzed by *Cinchona* alkaloid. Relative Gibbs free energies are shown in parentheses (kcal mol^{-1}).

In the resulting ion pair (**CI–IM1**), the $^{-}CH(CN)_2$ anion is reoriented to form a bidentate hydrogen-bond. The NBO charge accumulated on the $^{-}CH(CN)_2$ anion is predicated to be –0.834 *e*. The distance between N11 and H4 is 1.072 Å and the Wiberg bond index is 0.555, indicating the abstraction of H4 from the C1 atom and the formation of a N–H bond. As shown in Fig. 2(a), NBO analysis indicates that there exists an orbital interaction between the N2–C5 bonding orbital and the unfilled valence nonbonding orbital of the H4 atom [BD(σ)N2–C5→ Lp*(1)H4 (52.4 kcal mol^{-1})]. Furthermore, AIM calculations suggest a larger charge density ($\rho 1 = 0.296$ a.u.) and negative values of the Laplacian ($\nabla^2 \rho 1 = -1.525$) on (3,–1) BCP 1. These results indicate a stronger covalent interaction between the N11 and H4 with concentrated charge density along the bond path. However, the positive values of the Laplacian for BCPs 2 and 3 verify a relatively weaker hydrogen-bonding interaction between the protonated alkaloid and $^{-}CH(CN)_2$ anion (Fig. 2(b)). Table 1 shows reactivity indices for reactants, molecular complexes and intermediates. Compared with free malononitrile, the nucleophilicity index of **CI–COM** increases from –0.40 to 2.80 eV. The higher value for **CI–IM1** (4.32 eV) indicates that the $^{-}CH(CN)_2$ anion should be more reactive as a nucleophile for Michael addition of malononitrile to chalcone.

Table 1 Electronic chemical potential μ, chemical hardness η, global electrophilicity ω, and global nucleophilicity N for reactants, molecular complexes and intermediate

Species	μ [a.u.]	η [a.u.]	ω [eV]	N [eV]
Malononitrile (R1)	–0.1996	0.3214	1.69	–0.40
CI–COM	–0.1423	0.2010	1.37	2.80
CI–IM1	–0.1159	0.1424	1.28	4.32
R2	–0.1593	0.1923	1.79	2.46
A–COM	–0.1400	0.0919	2.90	4.35
N–COM	–0.1185	0.1007	1.90	4.81

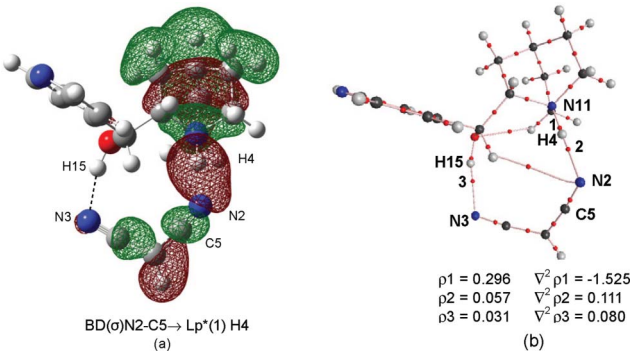

Fig. 2 (a) The visualization of the orbital interaction obtained by Gaussview. (b) Charge density (ρ) and corresponding Laplacian (∇^2 ρ) of selected bond critical points (BCP) for **CI-IM1** obtained by AIM.

Addition of malononitrile to model chalcone

Al(III)–CI complex catalyzed reaction. In initial investigation, a model system is employed to probe the possible reaction mechanism in detail. The experimental results indicate that quinine reacted *in situ* with aluminium reagents to form a reactive quinine–Al(III) complex, with the release of counter-ions (such as O*i*Pr^{-}).[3] The possible species, *i*PrOH, has been confirmed by NMR in the Strecker reaction.[25] Based on the experimental observations, a tetra-coordinated Al(III)-complex is assumed, in which model chalcone coordinates to the Al metal centre by the carbonyl O atom. Consequently, a ternary complex (**A–COM**) is formed initially at the reaction entrance (shown in Fig. 3).

For **A–COM**, the Al–O7 distance is predicted to be 1.862 Å. The C=C double bond for the carbonyl compound is longer than that of free **R2** (1.357 Å *vs.* 1.344 Å). The activation of carbonyl substrate can also be verified by an increased global electrophilicity ($\omega = 2.90$ eV). The $^{-}CH(CN)_2$ anion is positioned equatorially with the carbonyl moiety, with a distance of 1.778 Å between H4 and N2. NBO analysis indicates that the accumulated charge on the carbonyl substrate and $CH(CN)_2$ moiety are 0.058 *e* and –0.813 *e*, respectively. As a result, charge transfer will occur from the $CH(CN)_2$ moiety to the carbonyl substrate coordinated with the Al atom during the C–C bond formation step.

Next, the $^{-}CH(CN)_2$ anion approaches the carbonyl substrate, leading to the formation of C–C bond in **A–IM1** *via* the transition state **A–TS1**. Calculations predict the free energy barrier for this step to be 6.4 kcal mol^{-1}. For **A–TS1**, the distance between C1 and C10 is shortened remarkably from 3.449 to 2.328 Å, and

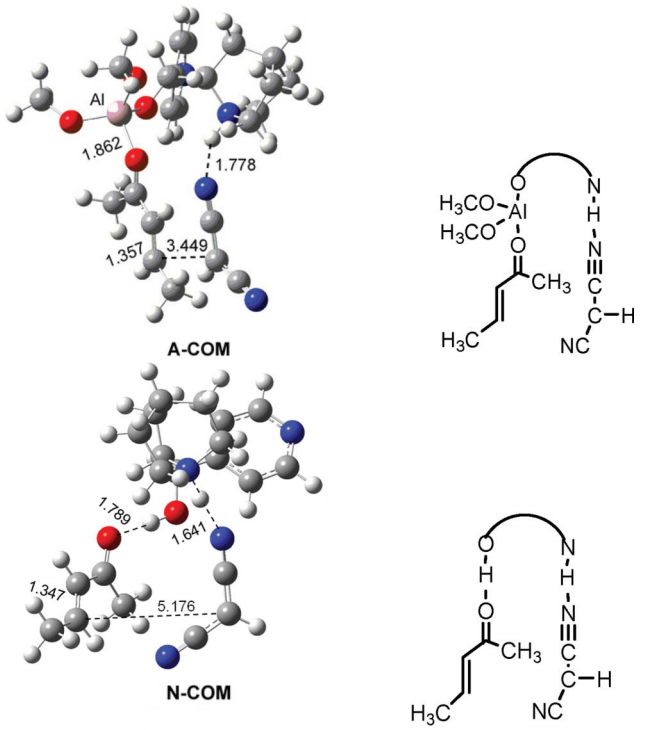

Fig. 3 Optimized geometries of molecular complexes for Al(III)-complex system (**A–COM**) and *Cinchona* alkaloid system (**N–COM**), respectively.

the increased interaction for forming the C–C bond can also be verified by a larger Wiberg bond index of 0.322 (0.036 for **A–COM**). Simultaneously, the C=C double bond of the carbonyl substrate moiety is further weakened, with the elongated C9–C10 bond length (from 1.357 to 1.399 Å) and the decreased Wiberg bond index (from 1.694 to 1.417).

The resultant intermediate **A–IM1** exhibits a zwitterionic character, with a larger net charge accumulated on the Al–carbonyl complex framework (0.859 *e*) and the dipole moment (7.835 D). The $CH(CN)_2$ group is stabilized by a weak hydrogen-bond between the H atom of the quinuclidine ring and N2 atoms, and the distance between the H4 and C9 atom is as much as 4.190 Å. In the following step, the C9–C10 bond rotates to force the larger bulky $CH(CN)_2$ group away from the quinuclidine ring and to force the protonated tertiary amine N atom of the quinuclidine moiety closer to the C9 atom, leading to the formation of **A–IM2**.

Then, the Michael addition reaction finishes by a proton transfer from N11 to C9 *via* the transition state **A–TS2**, producing a product-precursor **A–IM3**. The desired product would be formed by a direct dissociation of the Al–O bond. As shown in Fig. 4, this H transfer step is predicted to be the RDS with an energy barrier of 12.4 kcal mol^{-1} relative to **A–COM** at the reaction entrance. And the barrier is significantly smaller than that of the background reaction without catalyst (**B–TS**, 71.1 kcal mol^{-1}) (see Table S1 in the Supporting Information†). These results indicate that the Al^{III}-complex exhibits good catalytic ability for the Michael addition of malononitrile to chalcone.

***Cinchona* alkaloid catalyzed reaction.** In order to get a better understanding of the superior activation ability of the Al^{III}-complex as a Lewis acid for the carbonyl compounds observed in experiments,[3] and to compare the reaction mechanisms with

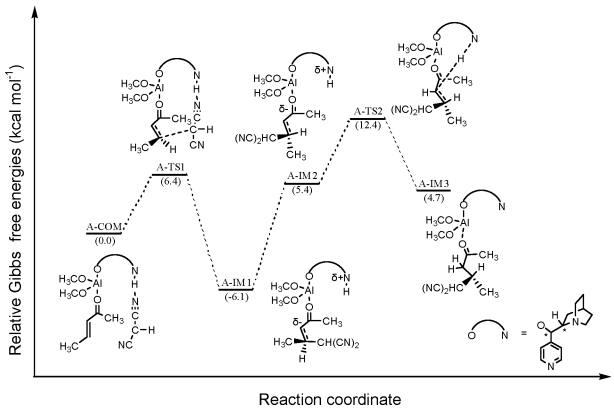

Fig. 4 Relative Gibbs free energy profile for the Michael addition of malononitrile to chalcone catalyzed by the Al^{III}-complex.

and without Al catalyst, we also analyze alternative mechanisms catalyzed by alkaloid alone.

Similarly, the reaction starts with the initial formation of the molecular complex **N–COM** (shown in Fig. 3), in which the carbonyl substrate interacts with the hydrogen atom of the hydroxyl group of *Cinchona* alkaloid with an (O)H···O distance of 1.789 Å. The geometry is loose with a longer distance between the C1 and C10 atoms (5.176 Å).

Next, a C–C bond is formed *via* the transition state **N–TS1**. The energy barrier for this step is predicted to be 18.8 kcal mol^{-1}, which is higher than that of the Al^{III}-complex system (6.4 kcal mol^{-1}). Reactivity index analysis also suggests a lower electrophilicity for the alkaloid complex than that of the Al^{III}-complex system (1.90 *vs.* 2.90 eV). Therefore, the Al^{III}-complex can be used as an effective Lewis acid catalyst for the activation of the carbonyl group, facilitating C–C bond formation.

IRC calculations and the following geometry optimizations as a continuation of the IRC path indicate that the proton transfer from the tertiary amine nitrogen atom (N11) of quinuclidine moiety to the carbonyl oxygen atom (O7) (rather than to the methylene carbon) occurs concomitantly with the formation of a C–C bond, producing the intermediate **N–IM1**. For **N–IM1**, the *Cinchona* alkaloid catalyst interacts with the enol isomer of the Michael addition product with a H4–N11 distance of 1.722 Å. Calculations indicate that the direct proton migration in the enol isomer from the carbonyl oxygen atom (O7) to the methylene carbon (C9) can take place *via* a four-membered ring transition state (**TS2**) with a higher energy barrier of 44.8 kcal mol^{-1} (shown in Fig. 5). Another lower energy barrier (30.4 kcal mol^{-1}) transition state (**N–TS2**) is also found, in which H transfer is carried out with the aid of the hydroxyl group of the *Cinchona* alkaloid. Starting from **N–IM1**, the intermediate **N–IM2** is formed by a rotation around the H15–O7 bond with a small energy barrier of 1.8 kcal mol^{-1}. For **N–IM2**, the H4–O14 and H15–C9 distances are 1.939 and 3.130 Å, respectively. The weak hydrogen bonding between H15 and $CH(CN)_2$ moiety is also favorable for the stabilization of **N–IM2** (the H15–N2 distance is 2.320 Å). In the following step, a H transfer from the O14 to C9 atom takes place concomitantly with a proton migration from O7 to O14 *via* a concerted six-membered ring transition state **N–TS2**, producing a product-precursor **N–IM3**.

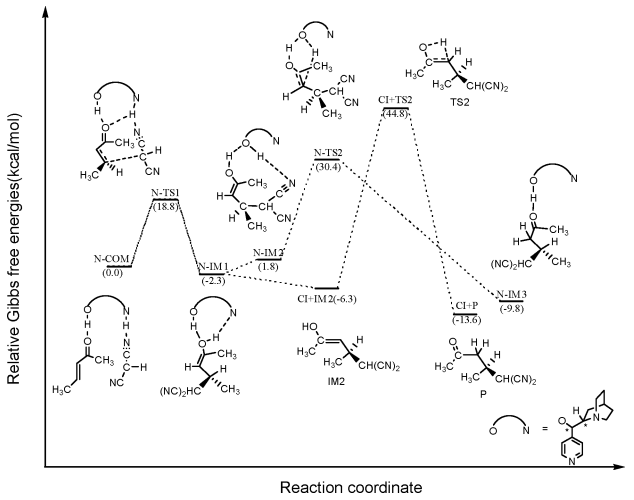

Fig. 5 Relative Gibbs free energy profile for the Michael addition of malononitrile to chalcone catalyzed by *Cinchona* alkaloid (CI).

Comparison of mechanisms catalyzed by Al(III)–*Cinchona* alkaloid complex and *Cinchona* alkaloid catalysts. Michael addition reactions between the malononitrile and α,β-unsaturated carbonyl compounds are characterized by the dominant nucleophile–electrophile interaction. The evolution of the electronic population along the reaction path is analyzed since significant electronic reorganization occurs in the formation of transition states.[26] Fig. 6 displays the evolution of charge on the $^{-}CH(CN)_2$ anion moiety and the O atom of the carbonyl group as the reaction proceeds along the IRC in the C–C bond formation step. The negative charge on the $^{-}CH(CN)_2$ anion moiety decreases for both *Cinchona* alkaloid and Al(III)–*Cinchona* alkaloid systems (Fig. 6(a)); while the negative charge increases on the carbonyl groups (see Fig. S1 in the Supporting Information†). These results indicate that there is a charge transfer from the $^{-}CH(CN)_2$ moiety to the carbonyl compounds in the C–C coupling step. The magnitude of charge variation for Al(III)–*Cinchona* alkaloid systems is narrower than that of the *Cinchona* alkaloid systems, and the net charge transfer of 0.255 *e* in **A–TS1** is smaller than that in **N–TS**(0.380 *e*). Hence, charge transfer between the $^{-}CH(CN)_2$ anion and the carbonyl group moiety is lessened in the presence of an Al catalyst.

During the formation of **A–IM1**, the negative charge accumulated on the carbonyl oxygen atom increases remarkably with the accompanying formation of the C–C bond (Fig. 3(b)), leading to the enhanced coordinating interaction between the O7 and Al atoms. These results can also be verified by an increased Wiberg bond index for the Al–O7 bond (from 0.277 to 0.363) and a shorter Al–O7 distance (from 1.862 to 1.773 Å) in **A–IM1**. As a result, the Michael addition product moiety with a –0.777 *e* charge could be stabilized by the Al^{III}-complex, leading to the key intermediate (**A–IM2**) necessary for the two-step mechanism. As opposed to the Al(III)–*Cinchona* alkaloid system, the negative charge of the $^{-}CH(CN)_2$ anion moiety decreased dramatically during the initial stage of the reaction in the CI system. Then, with the increased interaction between the O and H atoms during the formation of the C–C bond, the curve becomes gently smooth as a consequence of a retrodonation process. As shown in Fig. 6(a), the negative charges of the $^{-}CH(CN)_2$ moiety for **N–TS1** and **A–TS1** are –0.475 *e* and –0.557 *e*, respectively. The net charge accumulated on the O atom for the *Cinchona* alkaloid is smaller than that of the Al(III)–*Cinchona* alkaloid during the C–C bond formation process (see Fig. 3(b)). Then, the intermediate species with a more negative character could not be stabilized sufficiently by the hydroxyl group of the alkaloid during the formation of **N–IM1**. Consequently, the proton on the quinuclidine ring should transfer from the N11 to the O7 atom of the carbonyl moiety, forming an isomer of the Michael addition product (**N–IM1**).

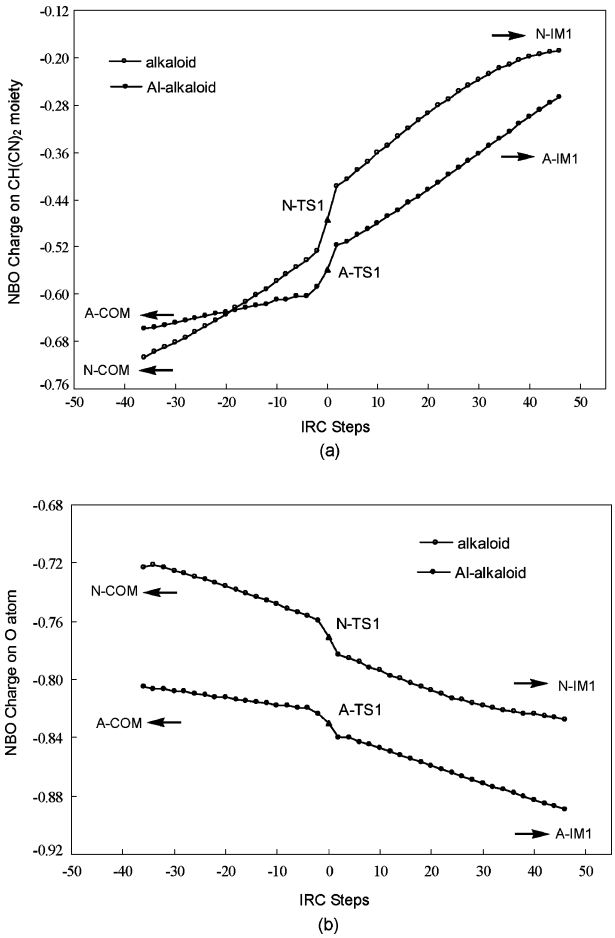

Fig. 6 Evolution of the charge populations in the formation of the C–C bond for the Michael addition reaction catalyzed by an *Cinchona* alkaloid and Al(III)–*Cinchona* alkaloid complex, respectively. (a) The evolution of the charge populations for the $CH(CN)_2$ moiety. (b) The evolution of charge accumulated on the O atom of the carbonyl compound moiety.

Stereoselectivities of products

Al(III)–quinine complex system. To explore the origin of the stereoselectivity of the Michael addition of malononitrile to chalcone, actual reaction systems are further considered (see Scheme 2). Herein, we assume that the chalcone has a *trans* double bond. Based on the results obtained from the model reaction above, theoretical calculations are performed at the ONIOM(B3LYP/6-311++G**:HF/STO-3G) level (see the Computational details section). Considering different coordination models, four kinds of possible tetra-coordinated Al(III)–quinine complexes were investigated in the present work (Scheme 4), in

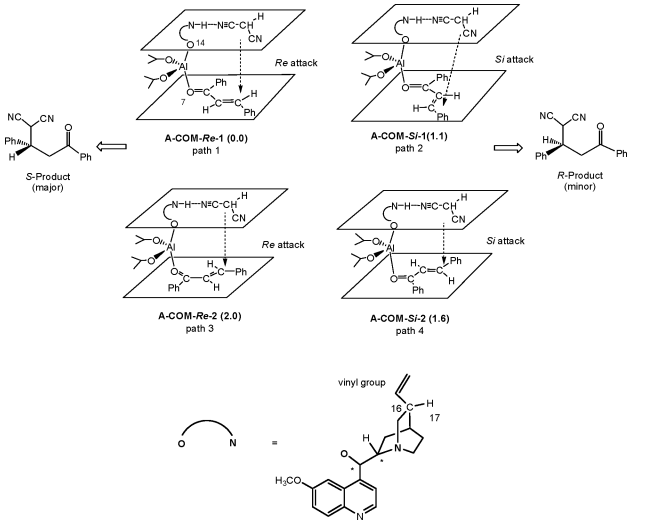

Scheme 4 Tetra-coordinated Al(III)–quinine complexes and their relative Gibbs free energy in parentheses (kcal mol^{-1}).

which the chalcone has two different conformations, s-*cis* and s-*trans*.

Calculations indicate that the tetra-coordinated Al(III)–quinine complexes have tetrahedral geometries, in which quinine ligands adopt an open conformation. The C=C double bonds of the vinyl groups are in a *cis* arrangement with the C16–H17 bond.[27] The quinoline and quinuclidine moieties are placed on either side of the O7–Al–O14 plane, respectively, and the bulky OMe group of the quinoline ring is positioned away from the chalcone substrate.

For **A–COM-*Re*-1** and **A–COM-*Si*-1**, the C=C bonds of the chalcones are on the same side of the quinuclidine moieties, while the phenyl group gets closer to the quinoline ring of the quinine ligands. The favorable π–π stacking effect between the quinuclidine ring and the phenyl group of the chalcones may be responsible for their lower relative energies compared to **A–COM-*Re*-2** and **A–COM-*Si*-2**. For **A–COM-*Re*-1** with the lowest energy, the C=C bond is s-*trans* to the carbonyl group in the chalcones and the phenyl group attached directly to the C=C double bond is placed far away from the isopropoxyl group, avoiding steric hindrance.

Four possible reaction pathways are explored starting with the corresponding Al(III)–quinine complexes shown in Scheme 4. Similarly, the step corresponding to the H atom transfer from the tertiary amine N atom to the chalcone is predicted to be the RDS. Optimized structures and relative Gibbs free energy for the key transition states are shown in Fig. 7 and Fig. S2 in the Supporting Information, respectively. The lowest energy reaction pathway (path 1) corresponds to the *Re* attack on chalcones, producing the *S*-product *via* the transition state **A–TS2-*Re*-1**, with energy barrier of 9.8 kcal mol^{-1}. For **A–TS2-*Re*-1**, the quinine moiety rotates around the O–Al bond to move the abstracted H atom of quinuclidine closer to the C atom on the chalcones. Simultaneously, the quinoline ring moves away from the chalcone substrates and isopropoxyl group, avoiding steric repulsion. Compared with **A–TS2-*Re*-1**, **A–TS2-*Re*-2** suffers more steric hindrance from the isopropoxyl group and therefore is kinetically unfavorable. Calculations predict that the energy barrier of **A–TS2-*Re*-2** is 3.1 kcal mol^{-1} higher than that of **A–TS2-*Re*-1**. The competing transition state to produce the *R* product is identified

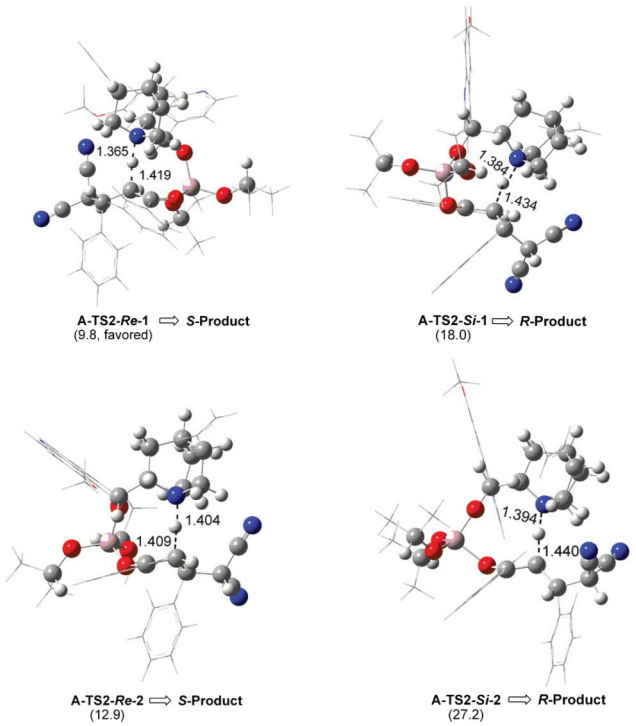

Fig. 7 Optimized geometries and relative Gibbs free energies (kcal mol^{-1}) of the transition states for the H transfer step in a Michael addition reaction catalyzed by an Al^{III}-complex.

as **A–TS2-*Si*-1**. Owing to steric repulsion between the bulky isopropoxyl and phenyl groups of the substrate, the activation barrier of 18.0 kcal mol^{-1} is higher than that *via* **A–TS2-*Re*-1** by 8.2 kcal mol^{-1}. These results indicate the predominant product has the *S* configuration, which is qualitatively in agreement with experimental observations. **A–TS2-*Si*-2** has the highest energy barriers (27.2 kcal mol^{-1}) due to repulsion of the phenyl groups of the substrate and the isopropoxyl group.

Quinine system. Furthermore, in order to gain insight into the superior stereoselective induction observed for Al(III)–quinine complexes, the asymmetric Michael addition reactions catalyzed by quinine alone are investigated. The geometries of the key transition states are also located on four reaction pathways as shown in Fig. 8 and Fig. S3, respectively. Comparing to the Al^{III}-complex systems, the initial molecular complexes are more axially flexible owing to the absence of bulky isopropoxyl groups. Calculations predict the energy barriers are about 8.3–16.0 kcal mol^{-1} for the C–C bond formation step (Table S2), which are higher than those of the corresponding step in Al^{III}-catalyzed systems (4.5–7.3 kcal mol^{-1}). For **N–TS1-*Re*-1**, the chalcone substrate is oriented by a hydrogen-bonding interaction of the hydroxyl group, and the H14–O7 distance is predicted to be 1.908 Å (see Fig. S3, ESI†). Simultaneously, the hydrogen atom on the tertiary nitrogen engages in the activation of the chalcone with an H4–O7 distance of 1.580 Å. As a result, the energy barrier for the C–C bond formation step is lower than those of other pathways.

The H transfer step is also predicated to be the RDS for the entire reaction (about 27.9–35.9 kcal mol^{-1}) catalyzed by quinine. The reaction pathway with the lowest energy barriers (27.9 kcal mol^{-1}, path 1) produces *S*-product *via* the transition state

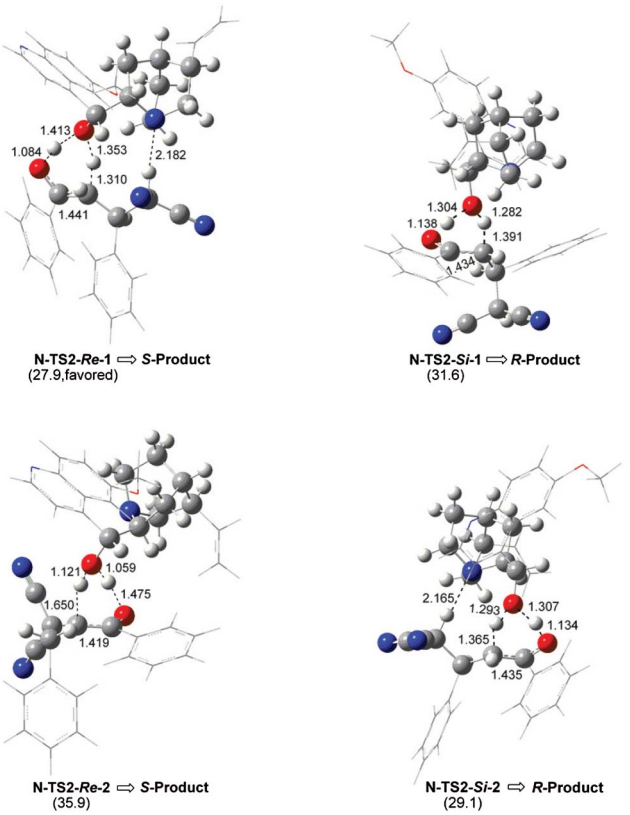

Fig. 8 Optimized geometries and relative Gibbs free energies (kcal mol^{-1}) of transition states for the H transfer step in a Michael addition reaction catalyzed by quinine.

N–TS2-*Re*-1. It is with the same stereochemistry as that of the experimentally observed predominant one. As shown in Fig. 8, the distance between the tertiary amine N atom and H atom of the $CH(CN)_2$ moiety in **N–TS2-*Re*-1** is 2.182 Å, indicating hydrogen bonding between them.[3] Simultaneously, the bulky quinoline ring moiety rotates around the C12–C13 bond to move away from the phenyl group of the chalcone, which may be of additional help to its stability. Different from the reaction mechanism for the Al-system, the activation barrier along path 2 *via* **N–TS2-*Si*-1** is higher than that of reaction path 4 *via* **N–TS2-*Si*-2** by 2.5 kcal mol^{-1}. The lack of hydrogen bonding between the quinuclidine nitrogen atom of quinine and the H atom in the $CH(CN)_2$ group may make **N–TS2-*Si*-1** slightly unstable. Calculations predict that the relative energy difference of the RDS for two competitive pathways (paths 1 and 4) is about 1.2 kcal mol^{-1}, which is smaller than that of the Al^{III}-complexes system (8.2 kcal mol^{-1}). These results are in good agreement with experimental observations that the chiral products with lower ee values were obtained when quinine alone was used as a catalyst.[3]

Therefore, an Al reagent with larger isopropoxyl groups combined with a chiral quinine alkaloid directs the coordination of the chalcone to adopt a certain conformation. As a result, a relatively rigid Al^{III}-complex with an ideal chiral environment can be formed (Scheme 5). Furthermore, the favorable π–π stacking effect between the quinuclidine ring of quinine and the phenyl group of the chalcone also plays a key role in the stabilization of the initial molecular complex. The steric repulsion between the phenyl group attached to the carbonyl group in chalcone and

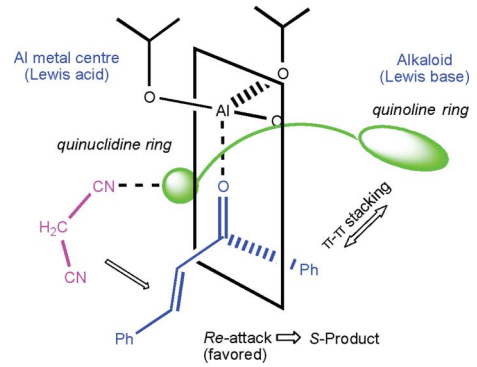

Scheme 5 Model proposed for predicting the stereochemistry of the Michael addition of malononitrile to chalcones catalyzed by Al(III)–quinine complex.

isopropoxyl groups of the Al^{III}-complex may also have a great effect on the enantioselectivity by increasing the hindrance of *Si* attack in transition states, identifying a kinetically favorable *Re*-attack on the chalcone. In the absence of Al reagent, the molecular complex is relatively flexible, and the steric repulsion between the phenyl group of chalcone and the quinoline ring of the quinine alkaloid makes the bulky quinoline ring move away from the chalcone substrate. As a result, *S*-product is formed with a lower energy barrier. These results are in agreement with experimental observations.[3]

Conclusion

DFT and ONIOM investigations on the mechanistic details of asymmetric Michael addition of malononitrile to chalcones catalyzed by *Cinchona* alkaloid–$Al(OiPr)_3$ reveal the following results:

1). A reactive tetra-coordinated Al(III)–*Cinchona* alkaloid complex with a relatively rigid structure can be formed, in which the Al^{III} acts as a more effective Lewis acid centre to activate the electrophile chalcone, while the tertiary amine in the *Cinchona* alkaloid works as a Lewis base to activate the nucleophile malononitrile. The rate-determining step (RDS) is predicted to be the H atom transfer from the tertiary amine to chalcone with an energy barrier of 12.4 kcal mol^{-1}.

2). The steric repulsion between the phenyl group attached to the carbonyl group in chalcone and the isopropoxyl groups of the Al^{III}-complex may play an important role in the control of the enantioselectivity. The π–π stacking effect between the quinuclidine ring of quinine and the phenyl group of chalcone may also favor the stabilization of the preferred molecular complex.

Acknowledgements

This work was supported by INHA University.

Notes and references

1 (*a*) P. Perlmutter, *Conjugate Addition Reactions in Organic Synthesis*, Pergamon, Oxford, 1992; (*b*) E. N. Jacobsen, A. Pfaltz and H. Yamamoto, *Comprehensive Asymmetric Catalysis*, Springer, New York, 1999, vol. III, pp. 1105; (*c*) M. P. Sibi and S. Manyem, *Tetrahedron*, 2000, **56**, 8033; (*d*) N. Krause and A. Hoffmann-Röder, *Synthesis*, 2001, 171; (*e*) O. M. Berner, L. Tedeschi and D. Enders, *Eur. J. Org. Chem.*, 2002,

1877; (*f*) R. Ballini, G. Bosica, D. Fiorini, A. Palmieri and M. Petrini, *Chem. Rev.*, 2005, **105**, 933; (*g*) S. B. Tsogoeva, *Eur. J. Org. Chem.*, 2007, 1701; (*h*) D. Almasi, D. A. Alonso and C. Nájera, *Tetrahedron: Asymmetry*, 2007, **18**, 299; (*i*) S. Sulzer-Mossé and A. Alexakis, *Chem. Commun.*, 2007, 3123.

2 (*a*) P. Kotrusz, S. Toma, H.-G. Schemalz and A. Adler, *Eur. J. Org. Chem.*, 2004, 1577; (*b*) S. Kanemasa and K. Itoh, *Eur. J. Org. Chem.*, 2004, 4741; (*c*) T. Okino, Y. Hoashi, T. Furukawa, X. Xu and Y. Takemoto, *J. Am. Chem. Soc.*, 2005, **127**, 119; (*d*) M. S. Taylor, D. N. Zalatan, A. M. Lerchner and E. N. Jacobsen, *J. Am. Chem. Soc.*, 2005, **127**, 1313; (*e*) E. P. Balskus and E. N. Jacobsen,, *J. Am. Chem. Soc.*, 2006, **128**, 6810; (*f*) J. Wang, H. Li, L. Zu, W. Jiang, H. Xie, W. Duan and W. Wang, *J. Am. Chem. Soc.*, 2006, **128**, 12652; (*g*) A. Carlone, S. Cabrera, M. Marigo and K. A. Jøgensen, *Angew. Chem., Int. Ed.*, 2007, **46**, 1101; (*h*) C. Guo, M.-X. Xue, M.-K. Zhu and L.-Z Gong, *Angew. Chem., Int. Ed.*, 2008, **47**, 3414; (*i*) Q. Zhu, L. Cheng and Y. Lu, *Chem. Commun.*, 2008, 6315; (*j*) A. Sato, M. Yoshida and S. Hara, *Chem. Commun.*, 2008, 6242; (*k*) B. Tan, X. Zhang, P. J. Chua and G. Zhong, *Chem. Commun.*, 2009, 779.

3 J. Shi, M. Wang, L. He, K. Zheng, X. Liu, L. Lin and X. Feng, *Chem. Commun.*, 2009, 4711.

4 For selected examples, see: (*a*) N. Halland, P. S. Aburel and K. A. Jøgensen, *Angew. Chem.*, 2003, **115**, 685, (*Angew. Chem., Int. Ed.*, 2003, **42**, 661); (*b*) H. Li, Y. Wang, T. Tang and L. Deng, *J. Am. Chem. Soc.*, 2004, **126**, 9906; (*c*) S. H. McCooey and S. J. Connon, *Angew. Chem.*, 2005, **117**, 6525, (*Angew. Chem., Int. Ed.*, 2005, **44**, 6367); (*d*) J. Ye, D. J. Dixon and P. S. Hynes, *Chem. Commun.*, 2005, 4481; (*e*) T. Ooi, D. Ohara, K. Fukumoto and K. Maruoka, *Org. Lett.*, 2005, **7**, 3195; (*f*) K. R. Knudsen, C. E. T. Mitchell and S. V. Ley, *Chem. Commun.*, 2006, 66; (*g*) J. M. Andres, R. Manzano and R. Pedrosa, *Chem.–Eur. J.*, 2008, **14**, 5116.

5 For selected examples, see: (*a*) J. Wang, H. Li, W. Duan, L. Zu and W. Wang, *Org. Lett.*, 2005, **7**, 4713; (*b*) M. Terada, H. Ube and Y. Yaguchi, *J. Am. Chem. Soc.*, 2006, **128**, 1454; (*c*) D. A. Evans, S. Mito and D. Seidel, *J. Am. Chem. Soc.*, 2007, **129**, 11583; (*d*) J. P. Malerich, K. Hagihara and V. H. Rawal, *J. Am. Chem. Soc.*, 2008, **130**, 14416.

6 For selected examples, see: (*a*) D. A. Evans and D. Seidel, *J. Am. Chem. Soc.*, 2005, **127**, 9958; (*b*) F. Wu, H. Li, R. Hong and L. Deng, *Angew. Chem.*, 2006, **118**, 961, (*Angew. Chem., Int. Ed.*, 2006, **45**, 947).

7 For selected examples, see: (*a*) S. Hanessian and V. Pham, *Org. Lett.*, 2000, **2**, 2975; (*b*) E. J. Corey and F.-Y. Zhang, *Org. Lett.*, 2000, **2**, 4257; (*c*) N. Halland, R. G. Hazell and K. A. Jørgensen, *J. Org. Chem.*, 2002, **67**, 8331; (*d*) T. Ooi, S. Fujioka and K. Maruoka, *J. Am. Chem. Soc.*, 2004, **126**, 11790; (*e*) B. Vakulya, S. Varga, A. Csámpai and T. Soós, *Org. Lett.*, 2005, **7**, 1967; (*f*) A. Prieto, N. Halland and K. A. Jørgensen, *Org. Lett.*, 2005, **7**, 3897.

8 (*a*) G. M. Sammis and E. N. Jacobsen, *J. Am. Chem. Soc.*, 2003, **125**, 4442; (*b*) Y.-C. Chen, D. Xue, J.-G. Deng, X. Cui, J. Zhu and Y.-Z. Jiang, *Tetrahedron Lett.*, 2004, **45**, 1555.

9 S. M. McElvain and J. W. Nelson, *J. Am. Chem. Soc.*, 1942, **64**, 1825.

10 (*a*) F. J. Weiberth and S. S. Hall, *J. Org. Chem.*, 1987, **52**, 3901; (*b*) I. Erdelmeier, C. Tailhan-Lomont and J.-C. Yadan, *J. Org. Chem.*, 2000, **65**, 8152.

11 (*a*) K. Itoh, Y. Oderaotoshi and S. Kanemasa, *Tetrahedron: Asymmetry*, 2003, **14**, 635; (*b*) M. S. Taylor and E. N. Jacobsen, *J. Am. Chem. Soc.*, 2003, **125**, 11204; (*c*) H. Yanagita, K. Kodama and S. Kanemasa, *Tetrahedron Lett.*, 2006, **47**, 9353; (*d*) T. Inokuma, Y. Nagamoto, S. Sakamoto, H. Miyabe, K. Takasu and Y. Takemoto, *Heterocycles*, 2009, **79**, 573; (*e*) Y. Hoashi, T. Okino and Y. Takemoto, *Angew. Chem.*, 2005, **117**, 4100, (*Angew. Chem., Int. Ed.*, 2005, **44**, 4032); (*f*) T. Inokuma, Y. Hoashi and Y. Takemoto, *J. Am. Chem. Soc.*, 2006, **128**, 9413; (*g*) X.-F. Li, L.-F. Cun, C.-X. Lian, L. Zhong, Y.-C. Chen, J. Liao, J. Zhu and J.-G. Deng, *Org. Biomol. Chem.*, 2008, **6**, 349; (*h*) L. Jing, J. Wei, L. Zhou, Z. Huang, Z. Li, D. Wu, H. Xiang and X. Zhou, *Chem.–Eur. J.*, 2010, **16**, 10955; (*i*) A. Russo, A. Perfetto and A. Lattanzia, *Adv. Synth. Catal.*, 2009, **351**, 3067; (*j*) C. G. Oliva, A. M. S. Silva, D. I. S. P. Resende, F. A. A. Paz and J. A. S. Cavaleiro, *Eur. J. Org. Chem.*, 2010, 3449.

12 D. Zhang, G. Wang and R. Zhu, *Tetrahedron: Asymmetry*, 2008, **19**, 568.

13 S. Kanemasa and K. Itoh, *Eur. J. Org. Chem.*, 2004, 4741.

14 K. N. Houk and Paul H. Cheong, *Nature*, 2008, **455**, 309.

15 (*a*) D. Gryko, M. Zimnicka and R. Lipiński, *J. Org. Chem.*, 2007, **72**, 964; (*b*) F. Ban, K. N. Rankin, J. W. Gauld and R. J. Boyd, *Theor. Chem. Acc.*, 2002, **108**, 1.

16 (*a*) A. D. Becke, *J. Chem. Phys.*, 1993, **98**, 5648; (*b*) C. Lee, W. Yang and R. G. Parr,, *Phys. Rev. B*, 1988, **37**, 785.

17 (*a*) F. Maseras and K. Morokuma, *J. Comput. Chem.*, 1995, **16**, 1170; (*b*) S. Humbel, S. Sieber and K. Morokuma, *J. Chem. Phys.*, 1996, **105**, 1959; (*c*) T. Matsubara, S. Sieber and K. Morokuma, *Int. J. Quantum Chem.*, 1996, **60**, 1101; (*d*) M. Svensson, S. Humbel, R. D. J. Froese, T. Matsubara, S. Sieber and K. Morokuma, *J. Phys. Chem.*, 1996, **100**, 19357; (*e*) M. Svensson, S. Humbel and K. Morokuma, *J. Chem. Phys.*, 1996, **105**, 3654; (*f*) S. Dapprich, I. Komáromi, K. S. Byun, K. Morokuma and M. J. Frisch, *THEOCHEM*, 1999, **461**, 1; (*g*) T. Vreven and K. Morokuma, *J. Comput. Chem.*, 2000, **21**, 1419.

18 *Gaussian 03, Revision B.05*, M. J. Frisch, G. W. Trucks, H. B. Schlegel, G. E. Scuseria, M. A. Robb, J. R. Cheeseman, J. A. Montgomery, Jr., T. Vreven, K. N. Kudin, J. C. Burant, J. M. Millam, S. S. Iyengar, J. Tomasi, V. Barone, B. Mennucci, M. Cossi, G. Scalmani, N. Rega, G. A. Petersson, H. Nakatsuji, M. Hada, M. Ehara, K. Toyota, R. Fukuda, J. Hasegawa, M. Ishida, T. Nakajima, Y. Honda, O. Kitao, H. Nakai, M. Klene, X. Li, J. E. Knox, H. P. Hratchian, J. B. Cross, V. Bakken, C. Adamo, J. Jaramillo, R. Gomperts, R. E. Stratmann, O. Yazyev, A. J. Austin, R. Cammi, C. Pomelli, J. W. Ochterski, P. Y. Ayala, K. Morokuma, G. A. Voth, P. Salvador, J. J. Dannenberg, V. G. Zakrzewski, S. Dapprich, A. D. Daniels, M. C. Strain, O. Farkas, D. K. Malick, A. D. Rabuck, K. Raghavachari, J. B. Foresman, J. V. Ortiz, Q. Cui, A. G. Baboul, S. Clifford, J. Cioslowski, B. B. Stefanov, G. Liu, A. Liashenko, P. Piskorz, I. Komaromi, R. L. Martin, D. J. Fox, T. Keith, M. A. Al-Laham, C. Y. Peng, A. Nanayakkara, M. Challacombe, P. M. W. Gill, B. Johnson, W. Chen, M. W. Wong, C. Gonzalez, J. A. Pople, Gaussian, Inc., Wallingford, CT, 2003.

19 (*a*) C. Gonzalez and H. B. Schlegel, *J. Chem. Phys.*, 1989, **90**, 2154; (*b*) C. Gonzalez and H. B. Schlegel, *J. Phys. Chem.*, 1990, **94**, 5523.

20 (*a*) A. E. Reed, L. A. Curtiss and F. Weinhold, *Chem. Rev.*, 1988, **88**, 899–926; (*b*) A. E. Reed, R. B. Weinstock and F. J. Weinhold, *J. Chem. Phys.*, 1985, **83**, 735.

21 (*a*) L. R. Domingo and J. A. Sáez, *Org. Biomol. Chem.*, 2009, **7**, 3576; (*b*) L. R. Domingo, E. Chamorro and P. Pérez, *J. Org. Chem.*, 2008, **73**, 4615; (*c*) R. G. Parr, L. von Szentpály and S. Liu, *J. Am. Chem. Soc.*, 1999, **121**, 1922; (*d*) L. R. Domingo, M. J. Aurell, P. Pérez and R. Contreras, *Tetrahedron*, 2002, **58**, 4417; (*e*) R. G. Parr, L. von Szentpaly and S. Liu, *J. Am. Chem. Soc.*, 1999, **121**, 1922; (*f*) R. G. Parr and R. G. Pearson, *J. Am. Chem. Soc.*, 1983, **105**, 7512; (*g*) R. G. Parr and W. Yang, Density Functional Theory of Atoms and Molecules, Oxford University Press, New York, 1989.

22 The global electrophilicity index ω,[21c,d] which measures the stabilization energy when the system acquires an additional electronic charge ΔN from the environment, is given in terms of the electronic chemical potential μ and chemical hardness η by the following simple expression:[21e] $\omega[\mathrm{eV}] = (\mu^2/2\eta)$. Both quantities can be calculated in terms of the HOMO and LUMO electron energies, ε_H and ε_L, as $\mu \approx (\varepsilon_H + \varepsilon_L)/2$ and $\eta \approx (\varepsilon_L - \varepsilon_H)$, respectively.[21f,g] The nucleophilicity index N,[21b] based on the HOMO energies obtained within the Kohn–Sham scheme, is defined as $N = E_{\mathrm{HOMO(Nu)}} - E_{\mathrm{HOMO(TCE)}}$.[21b] The nucleophilicity is taken relative to tetracyanoethylene (TCE) as a reference, because it has the lowest HOMO energy in a large series of molecules already investigated in the context of polar cycloadditions.

23 M. Cossi, G. Scalmani, N. Rega and V. Barone, *J. Chem. Phys.*, 2002, **117**, 43.

24 R. F. W. Bader, *Atoms in Molecules A Quantum Theory*, Oxford University Press, Oxford, 1990.

25 J. Wang, W. T. Wang, W. Li, X. L. Hu, K. Shen, C. Tan, X. H. Liu and X. M. Feng, *Chem.–Eur. J.*, 2009, **15**, 11642.

26 Y. Hannachi, J. Mascetti, A. Stirling and I. Pápai, *J. Phys. Chem. A*, 2003, **107**, 6708.

27 T. Bürgi and A. Baiker, *J. Am. Chem. Soc.*, 1998, **120**, 12920.